Volume 12, Issue 3, Page 72-77, 2023 https://doi.org/10.46810/tdfd.1294107 Research Article

BİNGÖL ÜNİVERSİTESİ

Türk Doğa ve Fen Dergisi
Turkish Journal of Nature and Science

www.dergipark.gov.tr/tdfd

Synthesis of TiO_2 Nanotubes and Examination of Photodiode Device Properties

Lütfi Bilal TAŞYÜREK[1*]

[1] Malatya Turgut Ozal University, Darende Bekir Ilicak V.H.S., Department of Opticians, Malatya, Türkiye
Lütfi Bilal TAŞYÜREK ORCID No: 0000-0003-0607-648X

**Corresponding author: bilaltasyurek@gmail.com*

(Received: 08.05.2023, Accepted: 22.08.2023, Online Publication: 27.09.2023)

Keywords
TiO_2, Nanotubes, Photodiodes, Electrical characteristics

Abstract: In this study, titanium dioxide (TiO_2) nanotubes were produced by anodization method using glycerol-based electrolyte. Structural characterization was investigated with SEM images and XRD pattern. The rectifying properties of n-type semiconductor TiO_2 nanotubes were investigated. Current-voltage (I-V) measurements of the Pt/TiO_2 nanotubes/Ti device were made at room temperature, in the dark and under different illumination conditions. The basic diode parameters were calculated by using thermionic emission (TE), Cheung and Norde functions from the I-V measurements of the devices in dark conditions. The ideality factors and barrier height of the Pt/TiO_2 nanotubes/Ti device were calculated 1.25 and 0.91 eV, respectively by the TE method. According to the results obtained, the Pt/TiO_2 nanotubes contact has a rectifying feature. In addition, the photovoltaic properties of the devices were examined by making I-V measurements at illumination intensities between 30 and 100 mW/cm^2. As a result, it has been evaluated that the device can also be used as a photodiode.

TiO_2 Nanotüplerin Sentezi ve Fotodiyot Aygıt Özelliklerinin İncelenmesi

Anahtar Kelimeler
TiO_2, Nanotüpler, Fotodiyotlar, Elektriksel karakterizasyon

Öz: Bu çalışmada, gliserol bazlı elektrolit kullanılarak anotlama yöntemi ile titanyum dioksit (TiO_2) nanotüpler üretilmiştir. Yapısal karakterizasyon, SEM görüntüleri ve XRD deseni ile incelenmiştir. N-tipi yarı iletken özellik gösteren TiO_2 nanotüplerin doğrultucu özellikleri incelenmiştir. Pt/TiO_2 nanotüpler/Ti cihazının akım-voltaj (I-V) ölçümleri oda sıcaklığında, karanlıkta ve farklı aydınlatma koşullarında yapılmıştır. Cihazların karanlık koşullarda I-V ölçümlerinden termiyonik emisyon (TE), Cheung ve Norde fonksiyonları kullanılarak temel diyot parametreleri hesaplanmıştır. TE yöntemi ile Pt/TiO_2 nanotüp/Ti cihazının idealite faktörleri ve bariyer yüksekliği sırasıyla 1,25 ve 0,91 eV olarak hesaplanmıştır. Elde edilen sonuçlara göre Pt/TiO_2 nanotüp kontağı doğrultucu özelliğe sahiptir. Ayrıca 30 ile 100 mW/cm^2 arasındaki aydınlatma şiddetlerinde I-V ölçümleri yapılarak cihazların fotovoltaik özellikleri incelenmiştir. Sonuç olarak cihazın fotodiyot olarak da kullanılabileceği değerlendirilmiştir.

1. INTRODUCTION

Metal oxides are used as interface layer to improve the electrical parameters of photodiodes. Photodiodes are sensitive to high-energy particles and photons. Thus, they convert light into electric current and find a wide place in optoelectronic technology. If the luminous energy exceeds the band gap energy of the semiconductor layer, electron-hole pairs are formed. When these pairs drift in opposite directions, a photocurrent is formed [1]. Titanium dioxide (TiO_2) thin films are widely used in solar cells [2], gas sensors [3], photocatalysis [4], etc., due to their electrical and optical properties. It is an n-type semiconductor suitable for various applications such as TiO_2 has three different crystal structures as rutile, anatase and brookite, with an indirect band gap of 3.0-3.2 eV. Thanks to this feature, its chemical, electrical and optical properties can be adapted for various applications [5]. In addition, TiO_2 is non-toxic and has a high dielectric constant and photocatalytic activity, increasing research opportunities.

Due to their properties, photodiodes have been investigated by many researchers to improve their performance [6], [7]. The electrical parameters of diodes using metal oxide nanostructures at their interfaces can be affected by the oxide layer [8]. Research has been carried out on diodes using TiO_2 as an interfacial [9].

While the values of the ideality factor and barrier height of the structure in dark conditions have been investigated, they have not been sufficiently investigated in illuminated conditions.

Despite many studies on TiO_2, the development of new materials for high-efficiency optoelectronic structures and their modeling remain hot research topics for current technologies. Thanks to their porous structure, TiO_2 nanoparticles provide large contact areas to adsorb dye molecules. This provides fast electron transfer and a large number of electrons [10]. Grain boundaries can cause photocurrent loss and lead to electron recombination in the near infrared region, which can result in loss of light absorption [11]. As an alternative to TiO_2 nanoparticles, TiO_2 nanotubes have been recognized as a promising option for photovoltaic applications. TiO_2 nanotubes attract attention with their features such as high surface/volume ratio, low cost and easy synthesis. The tubular porous structure of nanotubes provides a wide range of applications for light adsorption [12]. For photovoltaic applications, TiO_2 nanotubes offer advantages such as increased light scattering, fast electron transport and reduction of trap zones [13].

Rectifying contacts formed between metal and semiconductor have been a subject of extensive research in electronics for decades. Depending on the metal used as the contact, a Schottky barrier may form at the metal-metal oxide nanotube interface. Thus, the Fermi level may decrease [5]. Liu and Chen calculated the barrier height for Ag/TiO_2 nanoparticle contacts in their study [14]. Ling et al. [15] and Kwon et al. [16] examined the hydrogen sensor application of Au/TiO_2 and Pt/TiO_2 Schottky barrier diodes respectively. Mao et al. reported increased hydrogen sensor sensitivity of Pd decorated Ag/TiO_2 nanotube Schottky barrier diodes [17].

In our study, TiO_2 nanotubes were synthesized by anodization method using glycerol-based electrolyte and their morphological properties were determined. The electrical properties of the Schottky contact were investigated by making current-voltage (I-V) measurements and using different methods. Recently, nanostructures have been more intensively investigated in the fields of photovoltaic applications. Therefore, TiO_2 nanotubes are expected to contribute to the literature in photodetectors and photosensing devices. Finally, TiO_2 will be recommended to possible future research areas for the development of nanotube-based photovoltaic applications. In this way, it will be ensured that new nanotubes will be the subject of research such as this one.

2. MATERIAL AND METHOD

Glycerol electrolyte-based anodization method was applied to produce TiO_2 nanotubes. The cleaning procedure of commercial pure Ti foil (99%) with a size of 10x25 mm^2 and a thickness of 0.1 mm was applied for 15 minutes in an ultrasonic bath in acetone, isopropyl alcohol and deionized (DI) water, respectively. After each step of the cleaning procedure, the Ti foils were dried with high purity nitrogen (N_2) gas. 0.5 *wt*% NH_4F was added to the glycerol solution containing 15 *wt*% H_2O and mixed with a magnetic stirrer for 15 minutes at 20 ºC. The solution prepared in a teflon beaker was placed in a thermostat bath at 20 ºC Pt mesh (99.9%, Sigma-Aldrich) as anode and Ti foil as cathode were placed in the solution at a distance of 2 cm from each other and 40 V voltage was applied for 2 hours with DC power supply. After the anodization process, the removed foil was washed with DI water and dried with N_2 gas. Thus, the synthesis of TiO_2 nanotubes, which will serve as the interface in the device design, was completed.

Finally, TiO_2 nanotubes were coated with 100 nm thick Pt metal by DC magnetron sputtering method with shadow mask to take I-V measurements. Pt electrodes help to conduct electric current. The schematic representation of the produced Pt/TiO_2 nanotubes/Ti devices and the measurement system is shown in Figure 1.

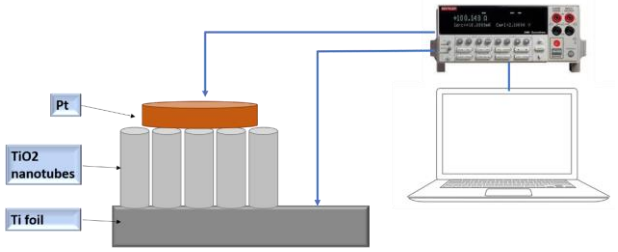

Figure 1. Schematic representation of Pt/TiO_2 nanotubes/Ti devices and measurement system

3. RESULTS

In Figure 2(A), the characteristic peaks of TiO_2 in x-ray difraction (XRD) pattern are 2θ=35.06º (100), 38.46º (002), 40.18º (101), 53.02º (102), 62.96º (110), 70.66º (103), 76.2º (112), 76.46º (201) seen [18]–[20]. After anodization, the surface morphology of the TiO_2 nanotubes was characterized by scanning electron microscopy (SEM). Nanotubes were formed on the entire surface of the Ti foil. It is clear that there is a difference between the diameters of the nanotubes in the SEM images and the nanotubes show a slight contraction in Figure 2 (B) and (C). The average nanotube diameters are between 160-170 nm. It shows that there is still some irregularity in the pore formation process. Some pores do not appear to have grown completely straight and some abrasion marks are visible on the surface. There are also undulations on the walls of the tubes that are not very rough, but not very rough. This is due to the self-organization of the nanotubes and diffusion through the pores. In addition, some anodization parameters need to be optimized [21], [22]. As seen from the SEM images, the nanotubes are homogeneously formed. However, the diameters of the tubes were not formed in the same dimensions. In order for the tube diameters to be the same, parameters such as anodization temperature, application voltage, application time can be optimized [23].

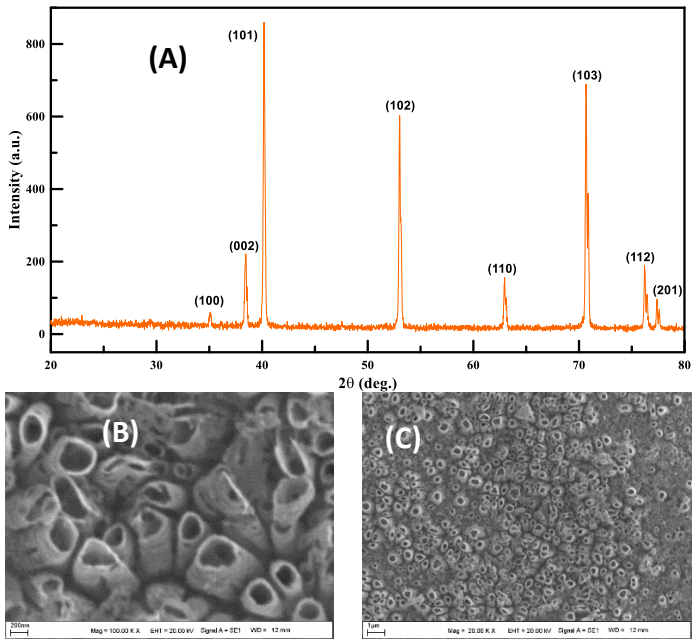

Figure 2. (A) XRD pattern and **(B-C)** SEM images of TiO_2 nanotubes

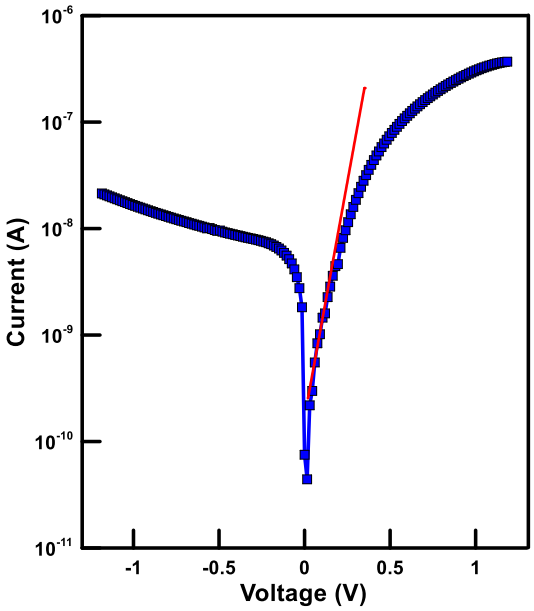

Figure 3. Semi-logarithmic I-V characteristic of Pt/TiO_2 nanotubes/Ti device at room tempeature

Thermionic emission theory (TE) in the linear region of the forward biased semi-logarithmic I-V plot (at low voltage) was used at both dark and illumination [24]–[26];

$$I = I_0 \left[exp\left(\frac{q(V-IRs)}{nkT}\right) - 1 \right] \quad (1)$$

where I_0 is the saturation current found given by;

$$I_0 = AA^*T^2\, exp\left(\frac{q\Phi_b}{kT} - 1\right) \quad (2)$$

The following equation is used to calculate the ideality factor (n) and the barrier height (Φ_b);

$$n = \frac{q}{kT}\frac{dV}{d(ln\, I)} \quad (3)$$

$$q\Phi_b = kT\, ln\left(\frac{AA^*T^2}{I_0}\right) \quad (4)$$

In the above equations; q is the charge of the electron, k Boltzmann constant (8.625×10^{-5} eVK^{-1}), A is the effective diode field (0.00785 cm^2), A^* Richardson constant ($A^*\sim1200$ $Acm^{-2}K^{-2}$ for TiO_2) [27] and T is temperature in Kelvin.

The n value (for ideal diodes, n=1) is calculated from the slope of the linear portion in the low voltage region in the forward direction of the semi-logarithmic I-V characteristic. For the Pt/TiO_2 nanotubes/Ti device, the n value calculated using the curve in Figure 3 is 1.25 and the Φ_b value is 0.95 eV at room temperature. The n value greater than one can be explained by the inhomogeneity of the barrier, the properties of the interface layer and the effect of series resistance (R_s) [28]–[30].

In order to understand the electrical characteristics of the Pt/TiO_2 nanotubes contact, it is not sufficient to examine only the linear region of the I-V graph in Figure 3. The R_s effect is seen, where the graph moves away from linearity in forward bias. One of the methods used to investigate the R_s effect is the Cheung functions [31]. The Cheung functions applied in the high voltage region are as follows;

$$\frac{dV}{d(ln\, I)} = \frac{nkT}{e} + IR_s \quad (5)$$

$$H(I) = V - n\left(\frac{kT}{q}\right) ln\left(\frac{I}{AA^*T^2}\right) = n\Phi_b + IR_s \quad (6)$$

The n value is calculated from the point where the dV/d(lnI)-I slope intersects the vertical axis and the Φ_b value is calculated from the point where the H(I)-I slope intersects the vertical axis in Figure 4. The R_s values are also calculated from the slopes of these graphs. The n value calculated from the dV/d(lnI)-I slope is 2.69 and the R_s value is 1867 kΩ. The Φ_b value calculated from the H(I)-I slope is 1.02 eV, and the R_s value is 1650 kΩ. Electrical parameters calculated by Cheung method were higher than those calculated by TE method. This is due to the fact that the I-V regions where the calculation is made are different. In addition, the R_s effect between Pt/TiO_2 nanotubes can be attributed to the increase in charge flow at high voltage and the inhomogeneity of the barrier height [32], [33].

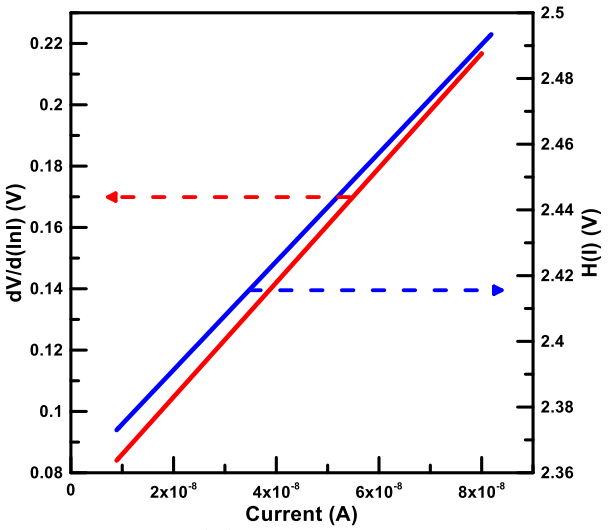

Figure 4. The graphs of of Pt/TiO_2 nanotubes/Ti device using Cheung functions at room temperature

Another method used to examine the R_s effect is the Norde functions [34]–[36] The linear and sloped region of the I-V graph in forward bias is used together to calculate the Norde functions and Φ_b and R_s values. Norde functions are given below;

$$F(V) = \frac{V}{\gamma} - \frac{kT}{q} ln\left(\frac{I(V)}{AA^*T^2}\right) \quad (7)$$

$$\Phi_b = F(V_0) + \frac{V_0}{\gamma} - \frac{kT}{q} \quad (8)$$

$$R_s = \frac{kT(\gamma - n)}{qI_{min}} \quad (9)$$

where γ is an integer greater than the ideality factor, I(V) is the current from the forward slope of the I-V curve, F(V0), V0 and Imin correspond to the minimum value of F(V). R_s =31332 kΩ and Φ_b =0.98 eV obtained with the help of Norde functions from the F(V)-V graphs shown in Figure 5 of Pt/TiO_2 nanotubes/Ti device. The results are generally in agreement with those obtained in previous methods. The main reason for the difference in the calculated values is that the Norde functions are applied to the entire forward-voltage region. It may also be due to the free carrier concentration caused by carriers at the interface between Pt/TiO_2 nanotubes [37]–[39].

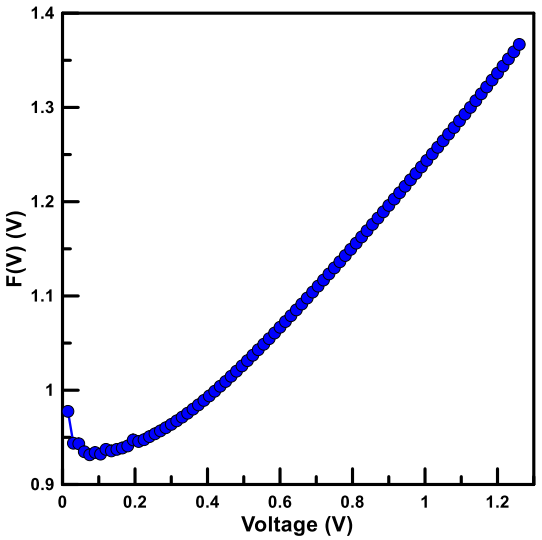

Figure 5. The graphs of of Pt/TiO_2 nanotubes/Ti device using Norde functions at room temperature

Figures 6 and 7 show the I-V characteristic of the Pt/TiO_2 nanotubes/Ti device at room temperature under 30, 40, 60, 80 and 100 mW/cm^2 light, respectively, in the dark. The n and Φ_b values at 100 mW/cm^2 illumination were calculated as 2.04 and 0.89 eV by using the I-V characteristic with TE method. The departure of the I-V plots under illumination from the linear region is attributed to the series resistance effect in the bending region . It is not fully linear as it is affected by the series resistance in the contact region [8]. It is understood from the graphs that they show rectifying properties. The saturation current (I_0) has small values (I_0=8.22 x 10^{-11} A). According to the reverse I-V graph, the increase in the current with the increase of the illumination intensity is explained by the photovoltaic behavior of the device. The movement of electron-hole pairs in the Pt/TiO_2 nanotubes contact is more pronounced in reverse bias than in forward bias. The energy of the photons is greater than the band gap energy, which can lead to the formation of electron-hole fences. The movement of these pairs can give useful information about the contact structure. The electron-hole pairs released along the contact can be separated by the electric field and move across the barrier [8], [40]–[42].

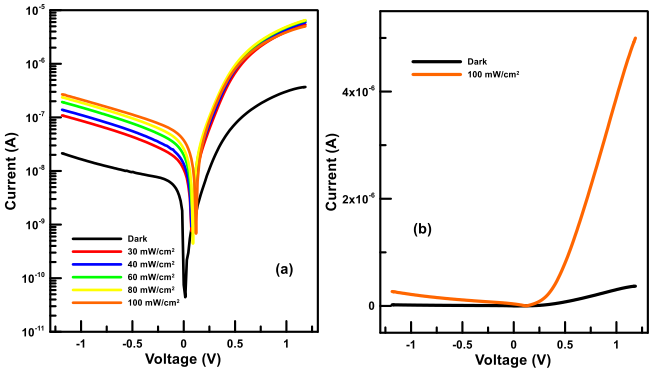

Figure 6. (a) Semi-logarithmic **(b)** lineer I-V grap of the Pt/TiO_2 nanotubes/Ti device in dark and different illuminations

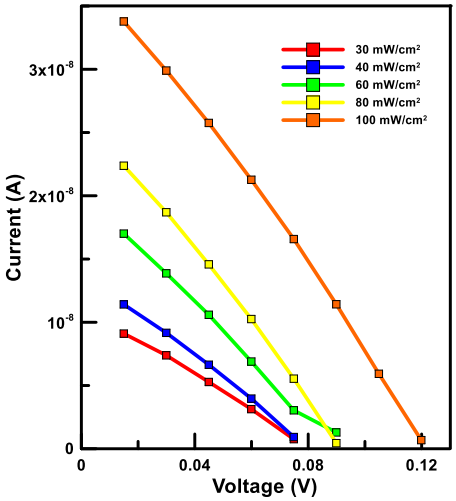

Figure 7. I-V grap of the Pt/TiO_2 nanotubes/Ti device in different illuminations

4. DISCUSSION AND CONCLUSION

In this study, TiO_2 nanotubes were produced by anodization method using glycerol-based electrolyte. XRD pattern and SEM images were examined to see the structural properties of TiO_2 nanotubes. The electrical characterization of TiO_2 nanotubes from the

nanostructured metal oxide group was investigated by three different methods (TE, Cheung and Norde functions). Photodiode performance and optical characterization were investigated under different lighting conditions. Then, Φ_b, n and R_s parameters were calculated from the I-V properties of the Pt/TiO_2 nanotubes contact. The n and Φ_b values of the Pt/TiO_2 nanotubes contact was measured as 1.25 and 0.91 eV, respectively by the TE method,. The results of I-V calculations by various methods were consistent. As a result, Pt/TiO_2 nanotubes showed rectifying properties. Photocurrent evaluation gave positive results for photodiode applications.

Acknowledgement

The author would like to thank Dr. Necmettin Kilinc from Inonu University for his help.

REFERENCES

[1] İ. Orak, "The performances photodiode and diode of ZnO thin film by atomic layer deposition technique," Solid State Communications, vol. 247, pp. 17–22, 2016.

[2] Y. Alivov, P. Xuan, and Z. Y. Fan, "TiO 2 nanotube height effect on the efficiency of dye-sensitized solar cells," 2011, doi: 10.1007/s11051-011-0627-1.

[3] N. Kılınç, E. Şennik, M. Işık, A. Ş. Ahsen, O. Öztürk, and Z. Z. Öztürk, "Fabrication and gas sensing properties of C-doped and un-doped TiO2 nanotubes," Ceramics International, vol. 40, no. 1, Part A, pp. 109–115, 2014, doi: https://doi.org/10.1016/j.ceramint.2013.05.110.

[4] M. Szkoda, K. Siuzdak, A. Lisowska-Oleksiak, J. Karczewski, and J. Ryl, "Facile preparation of extremely photoactive boron-doped TiO2 nanotubes arrays," Electrochemistry Communications, vol. 60, pp. 212–215, 2015.

[5] M. Yilmaz, B. B. Cirak, S. Aydogan, M. L. Grilli, and M. Biber, "Facile electrochemical-assisted synthesis of TiO2 nanotubes and their role in Schottky barrier diode applications," Superlattices and Microstructures, vol. 113, pp. 310–318, 2018.

[6] J. Cai, X. Chen, R. Hong, W. Yang, and Z. Wu, "High-performance 4H-SiC-based pin ultraviolet photodiode and investigation of its capacitance characteristics," Optics Communications, vol. 333, pp. 182–186, 2014.

[7] K. F. Brennan, J. Haralson II, J. W. Parks Jr, and A. Salem, "Review of reliability issues of metal-semiconductor-metal and avalanche photodiode photonic detectors," Microelectronics Reliability, vol. 39, no. 12, pp. 1873–1883, 1999.

[8] A. Karabulut, İ. Orak, and A. Türüt, "The photovoltaic impact of atomic layer deposited TiO2 interfacial layer on Si-based photodiodes," Solid-State Electronics, vol. 144, pp. 39–48, 2018.

[9] S. B. K. Aydin, D. E. Yildiz, H. K. Çavuş, and R. Şahingöz, "ALD TiO 2 thin film as dielectric for Al/p-Si Schottky diode," Bulletin of Materials Science, vol. 37, pp. 1563–1568, 2014.

[10] W.-Q. Wu et al., "Hydrothermal fabrication of hierarchically anatase TiO2 nanowire arrays on FTO glass for dye-sensitized solar cells," Scientific reports, vol. 3, no. 1, pp. 1–7, 2013.

[11] J. Maçaira, L. Andrade, and A. Mendes, "Review on nanostructured photoelectrodes for next generation dye-sensitized solar cells," Renewable and Sustainable Energy Reviews, vol. 27, pp. 334–349, 2013.

[12] X. Hou, K. Aitola, and P. D. Lund, "TiO2 nanotubes for dye-sensitized solar cells—A review," Energy Science & Engineering, vol. 9, no. 7, pp. 921–937, 2021.

[13] G. K. Mor, O. K. Varghese, M. Paulose, K. Shankar, and C. A. Grimes, "A review on highly ordered, vertically oriented TiO2 nanotube arrays: Fabrication, material properties, and solar energy applications," Solar Energy Materials and Solar Cells, vol. 90, no. 14, pp. 2011–2075, 2006.

[14] J. Liu and F. Chen, "Plasmon enhanced photoelectrochemical activity of Ag–Cu nanoparticles on TiO2/Ti substrates," Int. J. Electrochem. Sci, vol. 7, no. 9560, p. e9572, 2012.

[15] Y. Ling, F. Ren, and J. Feng, "Reverse bias voltage dependent hydrogen sensing properties on Au–TiO2 nanotubes Schottky barrier diodes," International Journal of Hydrogen Energy, vol. 41, no. 18, pp. 7691–7698, 2016, doi: https://doi.org/10.1016/j.ijhydene.2016.02.007.

[16] H. Kwon, J. H. Sung, Y. Lee, M.-H. Jo, and J. K. Kim, "Wavelength-dependent visible light response in vertically aligned nanohelical TiO2-based Schottky diodes," Applied Physics Letters, vol. 112, no. 4, p. 43106, 2018.

[17] [17] S. Mao et al., "High performance hydrogen sensor based on Pd/TiO2 composite film," International Journal of Hydrogen Energy, vol. 43, no. 50, pp. 22727–22732, 2018.

[18] J. M. Macak, L. V Taveira, H. Tsuchiya, K. Sirotna, J. Macak, and P. Schmuki, "Influence of different fluoride containing electrolytes on the formation of self-organized titania nanotubes by Ti anodization," Journal of electroceramics, vol. 16, no. 1, pp. 29–34, 2006.

[19] L. Özcan, T. Mutlu, and S. Yurdakal, "Photoelectrocatalytic degradation of paraquat by Pt loaded TiO2 nanotubes on Ti anodes," Materials, vol. 11, no. 9, p. 1715, 2018.

[20] X. Xiao, T. Tian, R. Liu, and H. She, "Influence of titania nanotube arrays on biomimetic deposition apatite on titanium by alkali treatment," Materials Chemistry and Physics, vol. 106, no. 1, pp. 27–32, 2007, doi: https://doi.org/10.1016/j.matchemphys.2007.05.014.

[21] R. Narayanan, T. Y. Kwon, and K. H. Kim, "TiO2 nanotubes from stirred glycerol/NH4F electrolyte: Roughness, wetting behavior and adhesion for implant applications," Materials Chemistry and Physics, vol. 117, no. 2–3, pp. 460–464, 2009, doi: 10.1016/j.matchemphys.2009.06.023.

[22] J. M. Macak et al., "TiO2 nanotubes: Self-organized electrochemical formation, properties and applications," Current Opinion in Solid State and Materials Science, vol. 11, no. 1–2, pp. 3–18, 2007,

doi: 10.1016/j.cossms.2007.08.004.
[23] E. Isik, L. B. Tasyurek, I. Isik, and N. Kilinc, "Synthesis and analysis of TiO2 nanotubes by electrochemical anodization and machine learning method for hydrogen sensors," Microelectronic Engineering, vol. 262, p. 111834, 2022, doi: https://doi.org/10.1016/j.mee.2022.111834.
[24] R. T. Tung, "Recent advances in Schottky barrier concepts," Materials Science and Engineering: R: Reports, vol. 35, no. 1–3, pp. 1–138, 2001.
[25] A. Turut, D. E. Yıldız, A. Karabulut, and İ. Orak, "Electrical characteristics of atomic layer deposited Au/Ti/HfO 2/n-GaAs MIS diodes in the wide temperature range," Journal of Materials Science: Materials in Electronics, pp. 1–11, 2020.
[26] S. M. Sze, Semiconductor devices: physics and technology. John wiley & sons, 2008.
[27] G. Rawat, H. Kumar, Y. Kumar, C. Kumar, D. Somvanshi, and S. Jit, "Effective Richardson constant of sol-gel derived TiO 2 Films in n-TiO 2/p-Si heterojunctions," IEEE Electron Device Letters, vol. 38, no. 5, pp. 633–636, 2017.
[28] D.-N. Bui, J. Mu, L. Wang, S.-Z. Kang, and X. Li, "Preparation of Cu-loaded SrTiO3 nanoparticles and their photocatalytic activity for hydrogen evolution from methanol aqueous solution," Applied surface science, vol. 274, pp. 328–333, 2013.
[29] Z. Çaldıran and L. B. Taşyürek, "The role of molybdenum trioxide in the change of electrical properties of Cr/MoO3/n-Si heterojunction and electrical characterization of this device depending on temperature," Sensors and Actuators A: Physical, p. 112765, 2021.
[30] A. R. Deniz, Z. Çaldıran, Ö. Metin, K. Meral, and Ş. Aydoğan, "The investigation of the electrical properties of Fe3O4/n-Si heterojunctions in a wide temperature range," Journal of colloid and interface science, vol. 473, pp. 172–181, 2016.
[31] S. K. Cheung and N. W. Cheung, "Extraction of Schottky diode parameters from forward current-voltage characteristics," Applied Physics Letters, vol. 49, no. 2, pp. 85–87, 1986.
[32] R. K. Gupta, K. Ghosh, and P. K. Kahol, "Fabrication and electrical characterization of Au/p-Si/STO/Au contact," Current Applied Physics, vol. 9, no. 5, pp. 933–936, 2009.
[33] A. TÜRÜT, "On current-voltage and capacitance-voltage characteristics of metal-semiconductor contacts," Turkish Journal of Physics, vol. 44, no. 4, pp. 302–347, 2020.
[34] H. Norde, "A modified forward I-V plot for Schottky diodes with high series resistance," Journal of Applied Physics, vol. 50, no. 7, pp. 5052–5053, 1979.
[35] A. Kocyigit, I. Orak, Z. Çaldıran, and A. Turut, "Current–voltage characteristics of Au/ZnO/n-Si device in a wide range temperature," Journal of Materials Science: Materials in Electronics, vol. 28, no. 22, pp. 17177–17184, 2017.
[36] A. Karabulut, A. Sarilmaz, F. Ozel, İ. Orak, and M. A. Şahinkaya, "A novel device fabricated with Cu2NiSnS4chalcogenide: Morphological and temperature-dependent electrical characterizations," Current Applied Physics, vol. 20, no. 1, pp. 58–64, 2020, doi: https://doi.org/10.1016/j.cap.2019.10.011.
[37] Y. S. Ocak, C. Bozkaplan, H. S. Ahmed, A. Tombak, M. F. Genisel, and S. Asubay, "Temperature dependent electrical characterization of RF sputtered MoS2/n-Si heterojunction," Optik, vol. 142, pp. 644–650, 2017.
[38] [38] A. Gencer Imer et al., "Interface controlling study of silicon based Schottky diode by organic layer," Journal of Materials Science: Materials in Electronics, vol. 30, pp. 19239–19246, 2019.
[39] E. Aldırmaz et al., "Cu-Al-Mn shape memory alloy based Schottky diode formed on Si," Physica B: Condensed Matter, vol. 560, pp. 261–266, 2019.
[40] A. A. M. Farag, H. S. Soliman, and A. A. Atta, "Analysis of dark and photovoltaic characteristics of Au/Pyronine G (Y)/p-Si/Al heterojunction," Synthetic metals, vol. 161, no. 23–24, pp. 2759–2764, 2012.
[41] A. G. Al-Sehemi, A. Karabulut, A. Dere, A. A. Al-Ghamdi, and F. Yakuphanoglu, "Photodiode performance and infrared light sensing capabilities of quaternary Cu2ZnSnS4 chalcogenide," Surfaces and Interfaces, vol. 29, p. 101802, 2022, doi: https://doi.org/10.1016/j.surfin.2022.101802.
[42] E. Özcan et al., "Fabrication of hybrid photodiode systems: BODIPY decorated cyclotriphosphazene covalently grafted graphene oxides," Inorganic Chemistry Frontiers, vol. 7, no. 16, pp. 2920–2931, 2020.